

MATHEMATICAL ANALYSIS

ROCKET-SLED MODEL STUDY OF PREDICTION TECHNIQUES FOR FLUCTUATING PRESSURES AND PANEL RESPONSE

Eric E. Ungar
Bolt Beranek and Newman Inc.
Cambridge, Massachusetts 02138

and

Ron E. Jewell and Harry J. Bandgren
National Aeronautics and Space Administration
George C. Marshall Space Flight Center
Huntsville, Alabama 35812

A description is given of an ongoing investigation dealing with the fluctuating pressures on aerospace vehicle surfaces, with associated panel responses, and with corresponding prediction techniques. The rocket-sled-mounted 1/10-scale model of the upper stages of Saturn V and the data acquisition system used in this study are described. Methods for predicting fluctuating pressures under turbulent boundary layers and subsonic separated flows are summarized and shown to yield predictions which are in reasonable agreement with measurements obtained on the test model.

INTRODUCTION

Predictions of the vibrations of aerospace vehicle structures due to aero-acoustic excitation are generally needed in the early design stages, primarily for the purpose of establishing preliminary design and test criteria. The problem of predicting the vibrations of a given structure may usually be divided into two steps: predicting the excitation, and determining the corresponding response. Much research effort has been devoted to both of these steps in the past decade, but although response-analysis techniques have been rather highly developed and extensively explored, much remains to be done before one can predict the aero-acoustic excitations with adequate confidence.

A compilation of techniques for the prediction of the fluctuating pressure environments of aerospace vehicles was undertaken about five years ago [1], but the general validity of these techniques has not been explored adequately. The fluctuating pressure data available from full-scale flight tests is very

limited; typically, only a very few microphones can be installed in a flight vehicle, and also telemetry limitations restrict the amount of data obtained from a given flight. Wind-tunnel studies tend to suffer from other shortcomings. Such studies usually involve small-scale models, for which the Reynolds numbers typically are two or more orders of magnitude smaller than for the actual vehicles; this discrepancy may provide improper information on fluctuating pressures. Also, the smallness of the models implies a requirement for microphones capable of sensing extremely high frequencies, and such sensors are not readily available. Flow interaction with tunnel walls also tends to distort the fluctuating pressures on vehicle surfaces, especially for the important transonic oscillating shock conditions.

In order to circumvent the problems associated with full-scale vehicle data acquisition and with the testing of small wind-tunnel models, a program of investigations has been undertaken, using a 1/10-scale model of the Saturn

N72-16843
(ACCESSION NUMBER)

(PAGES)

TMX 67490
(NASA CR OR TMX OR AD NUMBER)

(THRU)

63

(CODE)

32

(CATEGORY)

V vehicle mounted on a rocket-propelled sled, and making use of the facilities of the Air Force Missile Development Center, Holloman Air Force Base, New Mexico. The program involves several phases and objectives, including verification and improvement of prediction methods for fluctuating-pressure environments and corresponding responses of panels. This paper discusses some aspects of the aforementioned program, with emphasis on boundary-layer pressure data and predictions.

ROCKET-SLED MODEL TEST SYSTEM

Saturn V Model

The 1/10-scale model of Saturn V, mounted on the rocket sled, is shown in Fig. 1. This model incorporates only the upper parts of the Saturn V vehicle, from the command module (payload) down to about the forward half of the S-II stage. The total length of the model is about 20 ft; the forward 15 ft portion has been used for measurements, the aft 5 ft length contains a compartment for the instrumentation system and telemetry transmitters.

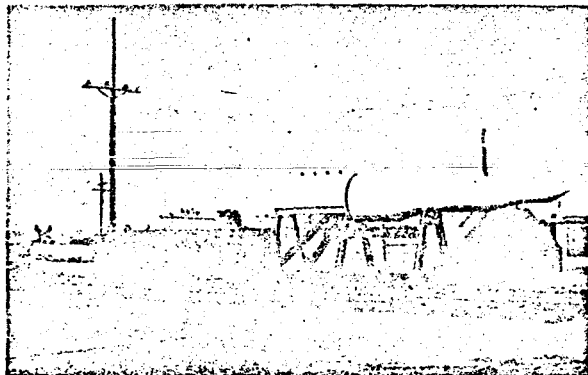


Figure 1
1/10-Scale Model of Saturn V
on Rocket Sled

The model, which was designed and fabricated by Brown Engineering on the basis of a concept proposed by NASA, has an aluminum cruciform primary structure, with ring-frames and stringers. The model's skin is 1/8 -in. thick aluminum plate; segments of the upper portion of the skin can be removed and replaced with thin panels. The thick skin-panels were used in early test runs, where the fluctuating pressure measurements were of primary interest; later runs involved vibration measurements on the thinner panels.

In order to get as much of the model as practical in front of aerodynamic disturbances caused by the leading edge of the test-sled and to minimize the effects of ground reflections, the forward part of the model is cantilevered over the end of the sled, and the model is quite high (about 5 ft) above the track. Also, pressure and vibration measurements were confined to only the upper parts of the model.

The model and support structure designs were reviewed by Holloman Air Force Base personnel, who also inspected these structures. The model also was subjected to a vibration test program, in order to verify its capability to withstand the severe vibration environment encountered during each rocket sled test run.

Rocket Sled Track and Propulsion

Test runs were carried out at the previously mentioned Holloman Air Force Base facility, on a dual-rail track which is in excess of 35,000 ft long. Both solid fuel and liquid fuel propulsion units were available for the program; Holloman personnel selected the propulsion systems for each test run. Although it would be ideal in each test run to attain a specific velocity and then to sustain that velocity for several seconds, this ideal could not be reached practically (because the liquid fuel rockets require a minimum acceleration of 0.5 g for fuel feed purposes). However, the 50 fps/sec velocity changes which could be obtained without much difficulty, proved to be more than adequate. Figure 2 shows the velocity profiles of the first four successful test runs.

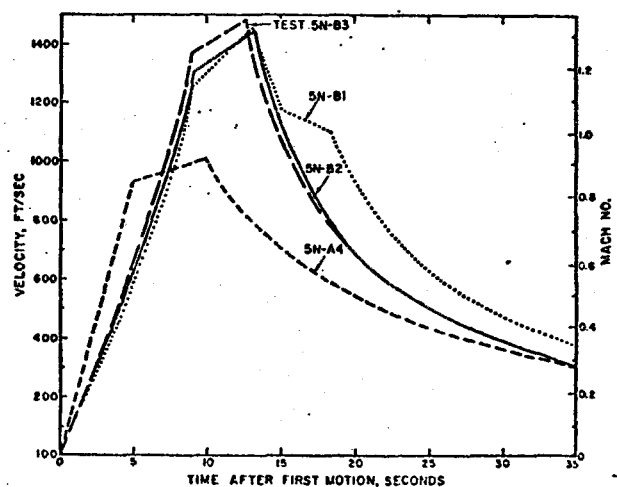


Figure 2 Velocity Histories For Four
Rocket Sled Tests

Instrumentation

The severe vibration environment associated with rocket sled test runs had to be taken into account in the selection of all transducers, which include lightweight high-g accelerometers, vibration-compensated microphones and differential pressure transducers. The transducers, amplifiers, voltage-controlled oscillators, mixer amplifiers and telemetry transmitters are mounted in the test model. Telemetry receivers, tape recorders, and discriminators are located at the central telemetry receiving facility of Holloman Air Force Base. Vehicle velocity information is obtained from position sensors located at fixed intervals along the track. A typical test run may involve twenty acoustic measurements, nine vibration measurements, five differential pressure measurements, and two velocity measurements; there are four telemetry transmitters and a total of 37 data channels.

End-to-end calibration of each data channel is accomplished two or three days before each test run, using an acoustic calibrator for each microphone, a small vibration shaker (monitored by a reference accelerometer) for each accelerometer, and a calibrated pressure source for the differential pressure sensors. On the day of the test, a known voltage signal is input to all voltage-controlled oscillators and transmitted to the receiving station, where it is recorded for later use as the data processing calibration signal.

During each test, the data is continuously transmitted to the telemetry receiving station, where it is simultaneously recorded on four tape recorders and on oscillographs. The oscillograms are reviewed visually immediately after each test, to uncover any anomalous behavior. (During removal of the instrumentation from the model, particular attention is given to the condition of any channels which might not have been functioning properly.) After each test, a second complete calibration is performed.

Data Reduction and Analysis

Oscillograph records for each test run are reviewed, together with velocity profiles, in order to identify the important phenomena and to select data samples to be subjected to detailed analysis. At the same time, decisions are also made on the type of data reduction desired for each data sample. The recorded data tapes are digitized and then processed by the Computation Laboratory at the NASA Marshall Space

Flight Center, and computer-plots and print-outs are prepared for review and analysis.

Computer-generated plots have been obtained, for example, of one-third octave band spectra, spectral densities, time-histories of one-third octave band and of overall levels, auto-correlations and cross-correlations, co-spectra and quadrature spectra, cross power spectral densities, and probability densities.

Some Early Operational Problems

Data to be analyzed by correlation techniques must be transmitted by constant bandwidth systems, with which Holloman personnel had limited experience. Improper operation of this telemetry system led to delay of the first scheduled test.

It was found in the first test run that the acoustic transducers generated a low frequency signal of large amplitude, which caused the charge amplifiers to saturate, thus leading to loss of much of the data. This problem was corrected in subsequent runs, by modifying the low-frequency response of the charge amplifiers.

In the first test (5N-A1) no attempt was made to obtain a sustained near-constant velocity period. The second test attempt failed because an engine malfunction at ignition damaged the propulsion system. In the second test (5N-A2), one of the engine thrust chambers developed a fracture, leading to premature thrust cut-off. The next run (5N-A3) was largely successful, except for a "sustain" velocity change which was twice as great as the desired value, due to improper propulsion programming. All later test runs to date (a total of four) have been entirely successful, and have yielded much useful data; additional test runs are planned for the near future.

FLUCTUATING PRESSURE PREDICTIONS AND MEASUREMENTS

Flow Regimes

The complexity of the total problem of predicting or analyzing fluctuating spectra may be reduced by first determining what flow regimes occur at various locations on the vehicle of interest (at a specified flight condition), and then establishing the fluctuating pressure characteristics associated with each flow regime. The flow regimes of greatest interest for the purpose of setting design and test criteria are: (1) turbulent boundary layers, (2) sep-

arated flow at discontinuities, (3) transonic oscillating shocks, (4) supersonic shock-induced separation at flares, (5) wake impingement, and (6) base flow.

The following paragraphs summarize prediction techniques, their basis, and some related rocket-sled test results for the first two of these flow regimes. It is anticipated that similar discussions of the other regimes will be presented in the future, when further data analysis and tests have been completed.

Fluctuating Pressures in Attached Turbulent Boundary Layers

Along long cylindrical stages of a launch vehicle, at locations which are more than one diameter downstream from interstage flares, the flow may be expected to be essentially free of strong pressure gradients. The flow at such locations may then be modeled as turbulent boundary layer flow on a flat plate.

Experiments on smooth flat plates indicate that the ratio of the root-mean-square fluctuating pressure p_{rms} to the wall shear stress τ in the flow is a slowly varying function of Mach number M ; at $M = 0$ this ratio is approximately 2, at $M = 5$ it is about 5, [2]. For a smooth flat plate with a fully developed boundary layer extending from the leading edge onward, Ref. [3] indicates that the shear stress τ at a distance X from the leading edge is related to the free-stream dynamic pressure q as

$$\tau/q \approx 0.060 (R_x)^{-1/5} \quad (1)$$

in terms of the Reynolds number

$$R_x = UX/\nu, \quad (2)$$

where U is the free-stream velocity, and ν the kinematic viscosity. (A surface may be considered smooth if its roughness elements are so small that they are buried in the laminar sublayer). If one introduces a linear interpolation for the Mach number dependence of p_{rms}/τ , one may write

$$\begin{aligned} p_{rms}/q &= (p_{rms}/\tau)(\tau/q) \\ &\approx (2 + 0.6M)(0.06)(\nu/MXc)^{1/5} \quad (3) \end{aligned}$$

where c represents the soundspeed. At a given location on a vehicle, and under given ambient conditions, ν/Xc is constant (dimensionless), and the foregoing expression may be used conveniently for estimation of p_{rms} .

Turbulent pressure spectra have been studied extensively; Fig. 3 represents a best fit to wind-tunnel data obtained by many investigators [4]. The peak of the spectrum occurs at a frequency

$$f_p \approx 0.16U/\delta^* \quad (4)$$

where δ^* is the boundary layer displacement thickness. In order to use Fig. 3 and Eq. (4) to predict the boundary layer pressure spectrum, one requires a prediction of δ^* . Such a prediction is available from Fig. 4, which has been taken from Ref. [4], and is based on correlation of empirical data.

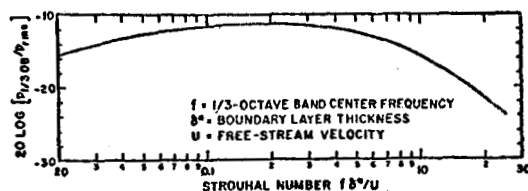


Figure 3

Nondimensional 1/3-Octave Band Spectrum of Pressure Fluctuations in Boundary Layer [1]

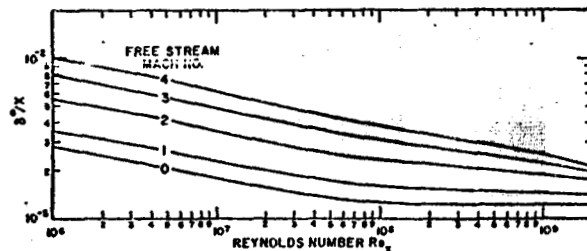


Figure 4

Dependence of Boundary Layer Thickness on Reynolds Number and Mach Number [4]

On the 1/10-scale Saturn V model, flush-mounted microphones were located near the front and rear ends of the SIV-B stage. This stage is located aft of a slightly (9-degree conical half-angle) flared part of the vehicle, and may be expected to be exposed to an attached turbulent boundary layer for most of the test sled velocities. The average distance to these microphones from the vehicle nose is about $X \approx 6$ ft. Using the values $c = 1100$ ft/sec, $\nu = 1.8 \times 10^{-4}$ ft²/sec and the air density $\rho = 0.066$ lb/ft³, which values apply at the 4000 ft altitude of the test track, one finds from Eq. (3) that p_{rms}/q varies by no more than 10% for Mach numbers between 0.2 and 1.4, and that in this Mach number range

$$p_{rms} \approx 0.005 q \approx (6.2 \text{ psf}) M^2$$

$$\approx (3000 \mu\text{bar}) M^2$$

One then may calculate the fluctuating pressure level FPL to be

$$\begin{aligned} \text{FPL} &\approx 20 \log (p_{rms}/p_{ref}) \\ &= 20 \log (p_{rms}/q) + 20 \log (q/p_{ref}) \\ &\approx 144 + 40 \log M \end{aligned} \quad (5)$$

in terms of the usual reference pressure $p_{ref} = 0.0002 \mu\text{bar}$.

From Fig. 4 one finds that for Mach numbers between 0.2 and 1.4 (for which R_x varies between 7 and 47 million), δ^*/X changes little and is equal to about 0.003. With this value and X as given above, Eq. (4) yields

$$f_p = 0.16 \text{ Mc}/\delta^* \approx 10,700 M \quad (6)$$

Figure 5 shows a plot of Eq. (5), together with data points from three microphones, obtained in two test runs. The prediction is seen to underestimate the bulk of the data by about 15 dB. However, the data points are found to fit rather well along a second curve corresponding to $p_{rms}/q = 0.02$. It appears that the fluctuating pressures at the microphone locations are greater than anticipated, probably due to the upstream turbulence. At supersonic speeds, reductions in p_{rms} occur due to attachment of the upstream flow and turbulence suppression. (Presence of a thick turbulent layer ahead of the S-IVB stage at subsonic speeds, and thinning of this layer at supersonic speeds is shown very clearly in Schlieren photographs, such as those given in Fig. 3 of Ref. [8]).

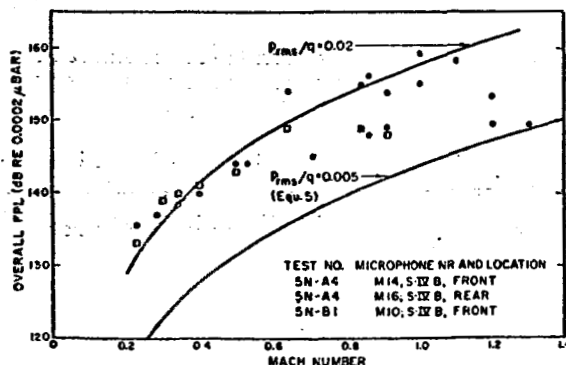


Figure 5

Levels of Fluctuating Pressure on S-IVB Stage of 1/10-Scale Model

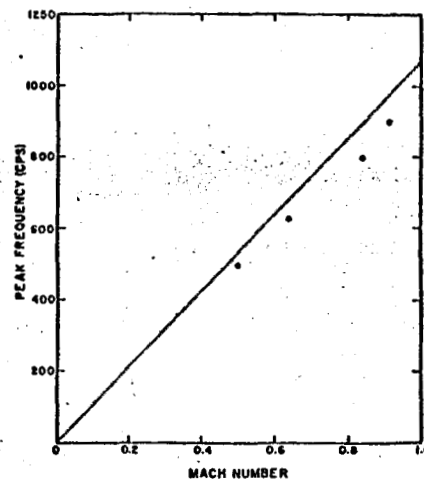


Figure 6

Center Frequency of 1/3-Octave Band Spectra of Fluctuating Pressures on S-IVB Stage of 1/10-Scale Model

Figure 6 shows the few presently available peak frequency data points (from microphone M14 on test 5N-A4), together with a plot of the relation $f_p = 10,700 M$. This relation, which is like Eq. (6), except for a ten times smaller numerical coefficient, fits the data much better than does Eq. (6). One concludes therefore that the boundary layer thickness at the microphone location is about ten times as great as that predicted for flat plates. This result is in agreement with the previously stated observation that the observed turbulence level greatly exceeds that expected for a flat plate; Schlieren photographs (e.g. Fig. 3 of Ref. [8]) also show a very thick boundary layer.

Measured and predicted one-third octave band spectra are compared in Fig. 7. This figure (which again shows data for microphone M14 in test 5N-A4 only) is presented in terms of a reduced fluctuating pressure level, defined as $\text{FPL}_R = \text{FPL} - 40 \log M$ and a reduced frequency, defined as $f_R = f/M$, in order to show also how well the data for different Mach numbers collapse (i.e., how good the approximations $p_{rms}/q = \text{constant}$ and $\delta^* = \text{constant}$ are - see Eqs. (5) and (6)). The agreement and collapse are seen to be quite good.

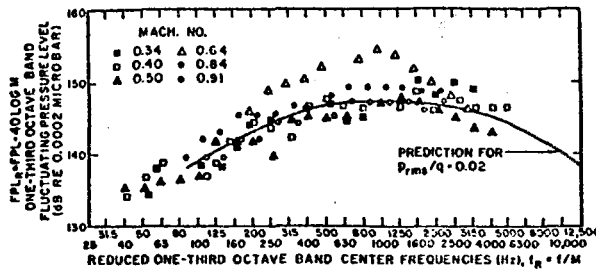


Figure 7
Fluctuating-Pressure Spectra on S-IVB
Stage of 1/10-Scale Model.

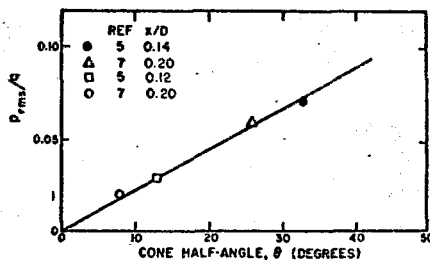


Figure 9
Effect of Cone Half-Angle (Flow Turning
Angle) on RMS Pressure Aft of Cone-
Cylinder Junction [1]

Subsonic Flow Separation Aft of Flares

At cone-cylinder junctions, the boundary layer experiences a strong pressure gradient (in subsonic flight). The level of pressure fluctuations then increases-owing to an increase in the rate of momentum entrainment necessary to overcome the pressure gradient.

Figures 8 and 9 have been assembled from the very limited available data. These figures show how p_{rms}/q increases with turning angle and decreases with distance downstream from the cone-cylinder junction, and are intended to be used for general prediction purposes in absence of better information. [1]

Figure 10 summarizes data obtained from microphones located behind flares; one set of microphones aft of the command module ($\theta = 30^\circ$, $x/D \approx 0.2$), the other on the S-II stage ($\theta = 17^\circ$, $x/D \approx 0.06$). For the former, Figs. 7 and 8 give $p_{rms}/q \approx 0.065$, for the latter $p_{rms}/q \approx 0.05$. Corresponding predic-

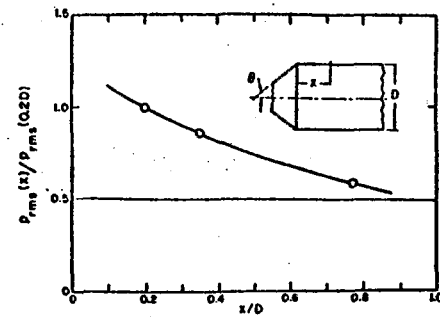


Figure 8
Decay of RMS Pressure With Distance
Downstream of Cone-Cylinder Junction.
Data Shown Are For $\theta = 33^\circ$,
From Ref. 6 [1].

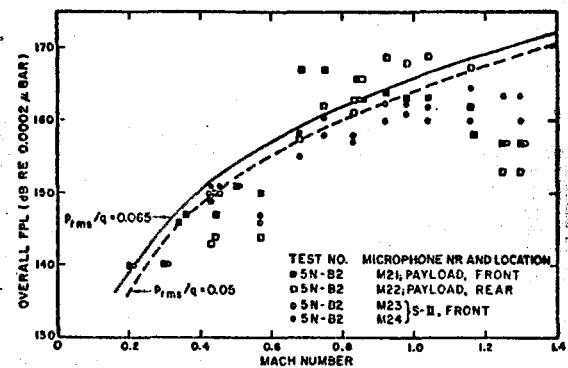


Figure 10
Levels of Fluctuating Pressure on
S-II Stage of 1/10-Scale Model

tion curves are shown in Fig. 9. Rather good agreement between predictions and data is evident, except for $M > 1$. At supersonic Mach numbers, one would once again expect p_{rms}/q to be reduced, because of the previously discussed suppression of turbulence.

SUMMARY AND CONCLUSIONS

A brief description has been presented of an ongoing program of investigation concerned with techniques for the prediction of aero-acoustic loads on aerospace vehicle surfaces and corresponding surface-structural responses. The rocket sled test model and associated instrumentation, which were used for the acquisition of fluctuating-pressure and panel response data have been discussed and have been shown to provide useful results.

Previously developed techniques for the prediction of fluctuating pressures associated with attached turbulent boundary layers and with

subsonic flow separation aft of flares have been summarized in easily used form. These techniques have been found to yield predictions which are in good agreement with data obtained from rocket sled model tests, provided that proper account is taken of the surface-flow conditions. It appears that the present state of the art permits one to arrive at reasonable fluctuating pressure predictions if one knows the flow regime which exists over the surface of interest, but that reliable predictions of the flow regimes generally can be obtained only on the basis of wind tunnel studies.

Some prediction techniques applicable to flow regimes other than the two mentioned above have also been developed [1], but their discussion has been omitted here, both for the sake of brevity and because analysis of the corresponding data is as yet incomplete. Further study of the available model and full-scale vehicle flight data is in progress, and additional tests are planned to supplement the existing information.

ACKNOWLEDGEMENT

The authors are indebted to Mr. David M. Green, of Brown Engineering, Huntsville, Alabama, who was responsible for the rocket sled instrumentation, for his description of the instrumentation systems and related calibration and analysis procedures. The help of Mr. Robert Abilock of Bolt Beranek and Newman Inc., Cambridge, Massachusetts, in data reduction and analysis is gratefully acknowledged.

REFERENCES

1. K.L. Chandiramani, S.E. Widnall, R.H. Lyon, P.A. Franken, "Structural Response to Inflight Acoustic and Aerodynamic Environments," Bolt Beranek and Newman Inc. Rept. 1417, July 1, 1966.
2. A.L. Kistler, "Surface Pressure Fluctuations Produced by Attached and Separated Supersonic Boundary Layers, AGARD Rept. 458, 1963.
3. H. Schlichting, *Boundary Layer Theory*, McGraw Hill Book Co., New York, 1960. Chapter XXI.
4. D.A. Bies, "A Review of Flight and Wind Tunnel Measurements of Boundary Layer Pressure Fluctuations and Induced Structural Response," NASA CR-626, 1966.
5. G.W. Jones and J.T. Foughner, "Investigation of Buffet Pressures on Models of Large Manned Launch Vehicle Configurations," NASA TN-D-1633, 1963.
6. J.D. Shelton, "Collation of Fluctuating Buffet Pressures for the Mercury/Atlas and Apollo/Saturn Configurations," NASA CR-66059, 1966.
7. D.R. Wiley and M.G. Seidl, "Aerodynamic Noise Tests on X-20 Scale Models," U.S. Air Force Flight Dynamics Laboratory AFFDL-TR-65-192.
8. H. Himmelblau, C.M. Fuller, T.D. Scharton, "Assessment of Space Vehicle Aeroacoustic-Vibration Prediction, Design, and Testing," NASA CR-1596, July 1970.